Bose-Einstein condensation of magnons and long-range order in coupled $S=1$ dimers on stacked triangular lattices

Bao Xu, Han-Ting Wang, and Yupeng Wang
Beijing National Laboratory for Condensed Matter Physics, Institute of Physics, Chinese Academy of Sciences, Beijing 100080, China
(Received 21 August 2007; published 2 January 2008)

The bond operator theory under the mean-field approximations is employed to investigate coupled spin-1 dimers on a stacked triangular lattice. The quantum phase transitions from the gapped spin liquid state to the ferromagnetic state or to the 120° three-sublattice antiferromagnetic state are studied with the idea of Bose-Einstein condensation of related magnons. A quantum phase transition from the spin liquid state to the quintuplet triangularly ordered state is also discussed. With the exchange coupling constants J_i $(i=0,1,2,3)$ extracted in connection with $Ba_3Mn_2O_8$, the magnetization curve, the temperature dependence of heat capacities, and the H-T (magnetic field–temperature) phase diagram are calculated. These results agree well with the experiments. The critical exponents near the critical fields H_{c1} and H_{c3} are calculated as $2/3$. The incommensurability is estimated as $\delta=0.02\pi$.

DOI: 10.1103/PhysRevB.77.014401 PACS number(s): 75.10.Jm, 75.50.−y, 05.30.Jp

I. INTRODUCTION

In 1956, Matsubara and Mastuda investigated the superfluidity of helium in the framework of a hard-core boson model by mapping it onto a quantum spin system in an external magnetic field.[1] The magnetic field and the magnetic order in the spin system correspond to the chemical potential and the off-diagonal long-range order in superfluid helium, respectively. After that, the idea of the Bose-Einstein condensation (BEC) of magnons was used to analyze the magnetization process of integer Heisenberg antiferromagnetic spin chains by Affleck[2] and of spin ladders by Giamarchi and Tsvelik.[3] In recent years, field-induced long-range order (LRO) in the plane perpendicular to the external magnetic field was observed in many gapped spin systems. Among them, the coupled $S=\frac{1}{2}$ dimer systems $TlCuCl_3$ (Ref. 4) and $BaCuSi_2O_6$ (Ref. 5) have been most extensively investigated. Besides the interesting LRO in the perpendicular plane, a magnetization plateau, a sharp peak in the temperature–magnetic field dependence of the specific heat, the phase diagram in the H (magnetic field)–T (temperature) plane, and the critical exponent α near the critical magnetic field were carefully studied. Theoretically, these interesting properties were attributed to the BEC of magnons and Bose-Einstein Hartree-Fock theory,[6,7] bond operator mean-field theory,[8,9] and quantum Monte Carlo simulations,[10,11] were employed to deal with them.

Unlike the spin-$\frac{1}{2}$ dimer systems, $Ba_3Mn_2O_8$ is an $S=1$ spin-dimer antiferromagnet.[12–14] The space group of this compound is trigonal $R\bar{3}m$. The Mn^{5+} ions form double-layered triangular lattices in the basal plane, which are stacked along the c axis with a periodicity of 3. Measurements of the magnetic susceptibility and the magnetization process showed that $Ba_3Mn_2O_8$ has a spin-singlet ground state with an excitation gap $\Delta=12.3$ K. The magnetization curve displays two plateaus at zero and at half of the saturation magnetization. At a given external magnetic field $9.5<H<25$ T, the temperature dependence of the specific heat shows anomalies, e.g., sharp peaks when $13\leqslant H\leqslant 23$ T, two peaks at $H=12$ T, and two shoulders at $H=24.5$ T. A magnetic phase diagram is given according to the specific heat measurements and is interpreted with the idea of Bose-Einstein condensation of magnons. The critical exponent α defined by $T_c\propto(H-H_c)^{\alpha}$ is determined to be $\alpha=0.39$.

The magnetization process was theoretically analysed by Uchida *et al.*[13] with a mean-field approximation. Some relations between the critical magnetic fields and the interaction parameters were obtained. In this paper, we employ the bond-operator theory[15] to investigate this coupled spin-1 dimer system. We mainly study the temperature- and field-dependent properties, for example, the phase diagram in the temperature-field plane, the specific heat, and the critical properties near the critical magnetic fields. For simplicity, we put the $S=1$ dimers on a hexagonal lattice. The model Hamiltonian reads

$$H=J_0\sum_{\vec{r}}\vec{S}_{\vec{r},1}\cdot\vec{S}_{\vec{r},2}+\frac{J_1}{2}\sum_{\vec{r},\vec{\beta}}(\vec{S}_{\vec{r},1}\cdot\vec{S}_{\vec{r}+\vec{\beta},2}+\vec{S}_{\vec{r},2}\cdot\vec{S}_{\vec{r}-\vec{\beta},1})$$
$$+\frac{J_2}{2}\sum_{\vec{r},\vec{\alpha}}(\vec{S}_{\vec{r},1}\cdot\vec{S}_{\vec{r}+\vec{\alpha},1}+\vec{S}_{\vec{r},2}\cdot\vec{S}_{\vec{r}+\vec{\alpha},2})+\frac{J_3}{2}\sum_{\vec{r},\vec{\alpha}}(\vec{S}_{\vec{r},1}\cdot\vec{S}_{\vec{r}+\vec{\alpha},2}$$
$$+\vec{S}_{\vec{r},2}\cdot\vec{S}_{\vec{r}+\vec{\alpha},1})-h\sum_{\vec{r}}(S^z_{\vec{r},1}+S^z_{\vec{r},2}). \quad (1)$$

Here, as shown in Fig. 1, $\vec{\alpha}$ and $\vec{\beta}$ denote nearest neighbors; J_0 is the exchange interaction between two spins in a dimer and J_i $(i=1,2,3)$ the exchange couplings of two spins in the nearest-neighbor dimers along the c direction and in the dimer plane, respectively. An external magnetic field $h=g\mu_B H$ is applied, with g the Landé factor and μ_B the Bohr magneton. For $Ba_3Mn_2O_8$, $g=1.98$. In comparison with the true geometry of $Ba_3Mn_2O_8$, J_1 can be regarded as an effective coupling between two double-layered triangular planes along the c direction. This simplification sounds reasonable since J_0 is much larger than J_i $(i=1,2,3)$.

In the rest of the paper, the bond-operator representation of a spin-1 dimer is applied to model (1) and the self-consistent equations are obtained under mean-field approximations in Section II. By studying the changes of the exci-

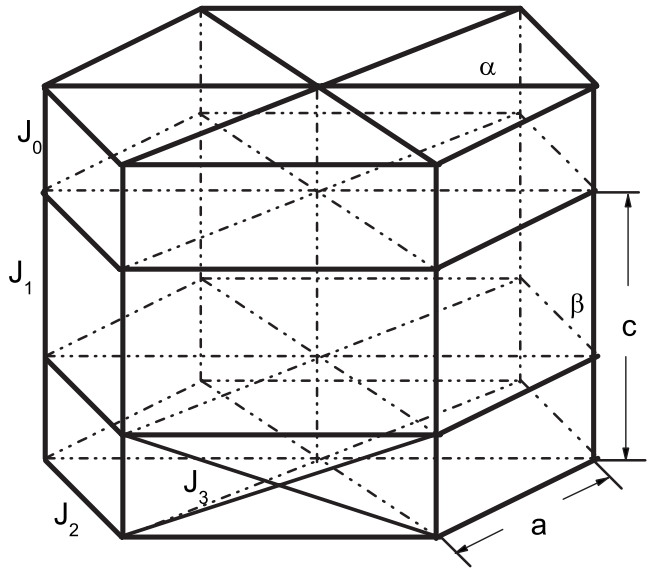

FIG. 1. Simplified geometry for $Ba_3Mn_2O_8$ with the spin-1 dimers placed on a stacked triangular lattice. The intradimer coupling J_0 is much larger than the interdimer interactions J_i ($i=1,2,3$).

tation gap with J_i, quantum phase transitions from the gapped spin liquid state to some ordered states are discussed in Section III. With the physical parameters extracted in relation to $Ba_3Mn_2O_8$, the magnetization, the thermodynamic properties, and the phase diagram are studied in Sec. IV. The effects of the true geometry of $Ba_3Mn_2O_8$, especially the incommensurability, are studied in Sec. V. A summary is given in Sec. VI.

II. BOND-OPERATOR REPRESENTATION AND THE EFFECTIVE HAMILTONIAN

For an $S=1$ spin dimer, the spin operators S_1 and S_2 can be represented by nine bosonic operators, which correspond to the nine eigenstates in Hilbert space, i.e., a singlet $|s\rangle = s^\dagger|\text{vac}\rangle$, three triplets $|t_{0,\pm1}\rangle = t^\dagger_{0,\pm1}|\text{vac}\rangle$, and five quintuplets $|q_{0,\pm1,\pm2}\rangle = q^\dagger_{0,\pm1,\pm2}|\text{vac}\rangle$:[16]

$$S^+_{1,2} = \pm\left(\frac{2}{\sqrt{3}}(s^\dagger t_{-1} - t_1^\dagger s) + \frac{1}{\sqrt{2}}(t_0^\dagger q_{-1} - q_0^\dagger t_{-1}) + \frac{1}{\sqrt{6}}(t_1^\dagger q_0 - q_1^\dagger t_0) + (t_{-1}^\dagger q_{-2} - q_2^\dagger t_1)\right) + \frac{1}{\sqrt{2}}(t_0^\dagger t_{-1} + t_1^\dagger t_0) + \frac{3}{\sqrt{6}}(q_1^\dagger q_0 + q_0^\dagger q_{-1}) + (q_2^\dagger q_1 + q_{-1}^\dagger q_{-2}),$$

$$S^-_{1,2} = (S^+_{1,2})^\dagger,$$

$$S^z_{1,2} = \pm\left(\frac{2}{\sqrt{6}}(s^\dagger t_0 + t_0^\dagger s) + \frac{1}{\sqrt{3}}(t_0^\dagger q_0 + q_0^\dagger t_0) + \frac{1}{2}(t_1^\dagger q_1 + q_1^\dagger t_1 + t_{-1}^\dagger q_{-1} + q_{-1}^\dagger t_{-1})\right) + \frac{1}{2}[n_{t,1} + n_{q,1} - n_{t,-1} - n_{q,-1} + 2(n_{q,2} - n_{q,-2})], \quad (2)$$

where $n_{\zeta,\sigma} = \zeta^\dagger_\sigma \zeta_\sigma$ with $\sigma = 0, \pm1$ for $\zeta = t$ and $\sigma = 0, \pm1, \pm2$ for $\zeta = q$. The single-occupancy condition requires $\Sigma_\zeta \Sigma_\sigma n_{\zeta,\sigma} + n_s = 1$. With the states of $|t_{0,\pm1}\rangle$ replaced by $|t_x\rangle = -(1/\sqrt{2})(|t_1\rangle + |t_{-1}\rangle)$, $|t_y\rangle = (i/\sqrt{2})(|t_1\rangle - |t_{-1}\rangle)$, and $|t_z\rangle = |t_0\rangle$, an alternative expression for the bond-operator representation was given by Brenig and Becker.[17]

Substituting the above representation into Hamiltonian (1) and introducing chemical potentials $\mu_{\vec{r}}$ to ensure single occupation at each dimer, we exactly obtain the model Hamiltonian in the bond-operator representation. In the singlet, triplet, and quintuplet states, the dimer has energies of $-2J_0$, $-J_0$, and J_0, respectively. In zero or small magnetic fields, we can project out the quintuplets for simplicity. The hard-core condition then becomes $\Sigma_\sigma n_{t,\sigma} + n_s = 1$. We solve this Hamiltonian by a mean-field approach.[15] Taking $\langle s_{\vec{r}}\rangle = s$, replacing the local constraint $\mu_{\vec{r}}$ by a global one μ, and making mean-field decouplings for the remaining four operator terms with $p_{\sigma,\vec{\Delta}} = \langle t^\dagger_{\vec{r},\sigma} t_{\vec{r}+\vec{\Delta},\sigma}\rangle$, $q_{\sigma,\vec{\Delta}} = \langle t^\dagger_{\vec{r},\sigma} t^\dagger_{\vec{r}+\vec{\Delta},\bar{\sigma}}\rangle$, $\sigma = 0, \pm1$, and $m = \langle S^z_{\vec{r},1} + S^z_{\vec{r},2}\rangle = \langle n_{t,1} - n_{t,-1}\rangle$, we get the diagonalized Hamiltonian after a Fourier-Bogoliubov transformation:

$$H = Ne_0 + \sum_{\vec{k}} \sum_\sigma \left(\alpha^\dagger_{\vec{k},\sigma}\alpha_{\vec{k},\sigma} + \frac{1}{2}\right)\omega_{\vec{k},\sigma}, \quad (3)$$

where e_0 is a constant independent of $\vec{k}$. The excitation spectra are

$$\omega_{\vec{k},\sigma} = \sqrt{A^2_{\vec{k}} - D^2_{\vec{k}}} + \sigma B_{\vec{k}}, \quad \sigma = \pm1,$$

$$\omega_{\vec{k},0} = \sqrt{C^2_{\vec{k}} - (2F_{\vec{k}})^2}, \quad (4)$$

with

$$A_{\vec{k}} = \mu + \frac{4}{3}s^2\mathcal{J}_{\vec{k}} + \frac{1}{2}[6p_{0,\vec{\alpha}}(J_2 + J_3)\gamma_{\vec{k},\alpha} + p_{0,\vec{\beta}}J_1\gamma_{\vec{k},\beta}],$$

$$B_{\vec{k}} = -h + \frac{1}{2}mJ,$$

$$D_{\vec{k}} = -\frac{4}{3}s^2\mathcal{J}_{\vec{k}} + \frac{1}{2}[6q_{0,\vec{\alpha}}(J_2 + J_3)\gamma_{\vec{k},\alpha} + q_{0,\vec{\beta}}J_1\gamma_{\vec{k},\beta}],$$

$$C_{\vec{k}} = \mu + \frac{4}{3}s^2\mathcal{J}_{\vec{k}} + \frac{1}{2}[6(p_{1,\vec{\alpha}} + p_{\bar{1},\vec{\alpha}})(J_2 + J_3)\gamma_{\vec{k},\alpha} + (p_{1,\vec{\beta}} + p_{\bar{1},\vec{\beta}})J_1\gamma_{\vec{k},\beta}],$$

$$F_{\vec{k}} = \frac{2}{3}s^2\mathcal{J}_{\vec{k}} + \frac{1}{2}[6q_{1,\vec{\alpha}}(J_2 + J_3)\gamma_{\vec{k},\alpha} + q_{1,\vec{\beta}}J_1\gamma_{\vec{k},\beta}],$$

where $J = J_1 + 6(J_2 + J_3)$, $\mathcal{J}_{\vec{k}} = 6(J_2 - J_3)\gamma_{\vec{k},\alpha} - J_1\gamma_{\vec{k},\beta}$, $\gamma_{\vec{k},\alpha} = \frac{1}{3}\cos(k_x a) + \frac{2}{3}\cos(\frac{1}{2}k_x a)\cos(\frac{\sqrt{3}}{2}k_y a)$, and $\gamma_{\vec{k},\beta} = \cos(k_z c)$. $\alpha^\dagger_{\vec{k},\sigma} = a_{\vec{k}}t^\dagger_{\vec{k},\sigma} + b_{\vec{k}}t_{-\vec{k},\bar{\sigma}}$ with $a_{\vec{k}} = \cosh\theta_{\vec{k}}$, $b_{\vec{k}} = \sinh\theta_{\vec{k}}$ and $\tanh\theta_{\vec{k}} = \frac{x_{\vec{k}}}{2} \pm \sqrt{\frac{x^2_{\vec{k}}}{4} - 1}$. For $\sigma = \pm1$, $x_{\vec{k}} = \frac{A_{\vec{k}}}{D_{\vec{k}}}$ and for $\sigma = 0$, $x_{\vec{k}} = \frac{C_{\vec{k}}}{F_{\vec{k}}}$.

The self-consistent equations are written as

$$s^2 = \frac{5}{2} - \frac{1}{N}\sum_{\vec{k}} \left[\frac{C_{\vec{k}}}{\omega_{\vec{k},0}}[n(\omega_{\vec{k},0}) + 1/2] + \frac{A_{\vec{k}}}{(\omega_{\vec{k},1} + \omega_{\vec{k},\bar{1}})/2} \sum_{\sigma\neq 0} \left(n(\omega_{\vec{k},\sigma}) + \frac{1}{2} \right) \right],$$

$$\mu = J_0 - \frac{1}{N}\sum_{\vec{k}} \left[\frac{A_{\vec{k}} + D_{\vec{k}}}{(\omega_{\vec{k},1} + \omega_{\vec{k},\bar{1}})/2} \sum_{\sigma\neq 0} \left(n(\omega_{\vec{k},\sigma}) + \frac{1}{2} \right) + \frac{C_{\vec{k}} - 2F_{\vec{k}}}{\omega_{\vec{k},0}}[n(\omega_{\vec{k},0}) + 1/2] \right] \frac{4}{3}\mathcal{J}_{\vec{k}},$$

$$m = \frac{1}{N}\sum_{\vec{k}} \sum_{\sigma\neq 0} \sigma n(\omega_{\vec{k},\sigma}),$$

$$p_{\sigma,\vec{\Delta}} = \frac{1}{N}\sum_{\vec{k}} \left[\frac{A_{\vec{k}}/2}{(\omega_{\vec{k},1} + \omega_{\vec{k},\bar{1}})/2} \sum_{\sigma\neq 0} \left(n(\omega_{\vec{k},\sigma}) + \frac{1}{2} \right) + \frac{n(\omega_{\vec{k},1}) - n(\omega_{\vec{k},\bar{1}})}{2} \right] \gamma_{\vec{k},\Delta}, \quad \sigma \neq 0,$$

$$p_{0,\vec{\Delta}} = \frac{1}{N}\sum_{\vec{k}} \frac{C_{\vec{k}}}{\omega_{\vec{k},0}} \left(n(\omega_{\vec{k},0}) + \frac{1}{2} \right) \gamma_{\vec{k},\Delta},$$

$$q_{\sigma,\vec{\Delta}} = \frac{1}{N}\sum_{\vec{k}} \frac{-D_{\vec{k}}/2}{(\omega_{\vec{k},1} + \omega_{\vec{k},\bar{1}})/2} \sum_{\sigma\neq 0} \left(n(\omega_{\vec{k},\sigma}) + \frac{1}{2} \right) \gamma_{\vec{k},\Delta},$$

$$q_{0,\vec{\Delta}} = \frac{1}{N}\sum_{\vec{k}} \frac{-2F_{\vec{k}}}{\omega_{\vec{k},0}} \left(n(\omega_{\vec{k},0}) + \frac{1}{2} \right) \gamma_{\vec{k},\Delta}, \tag{5}$$

where $\vec{\Delta} = \vec{\alpha}, \vec{\beta}$ and $n(x) = 1/(e^{\beta x} - 1)$ with $\beta = 1/k_B T$ and k_B the Boltzmann constant.

III. QUANTUM PHASE TRANSITIONS AT ZERO MAGNETIC FIELD

At zero magnetic field, the magnetization m is zero. Neglecting $p_{\sigma,\vec{\Delta}}$ and $q_{\sigma,\vec{\Delta}}$, we get three degenerate excitation spectra with $\omega_{\vec{k}} = \sqrt{\mu(\mu + \frac{8}{3}s^2\mathcal{J}_{\vec{k}})}$. Recalling that $\mathcal{J}_{\vec{k}} = 6(J_2 - J_3)\gamma_{\vec{k},\alpha} - J_1\gamma_{\vec{k},\beta}$ with $\gamma_{\vec{k},\alpha} = \frac{1}{3}\cos(k_x a) + \frac{2}{3}\cos(\frac{1}{2}k_x a)\cos(\frac{\sqrt{3}}{2}k_y a)$ and $\gamma_{\vec{k},\beta} = \cos(k_z c)$, we find that the lowest excitation (energy gap) is located at a $\vec{k}_c$ with $\gamma_{\vec{k}_c,\alpha} = -\frac{1}{2}$ and $\gamma_{\vec{k}_c,\beta} = 1$ for $J_2 - J_3 > 0$ and with $\gamma_{\vec{k}_c,\alpha} = 1$ and $\gamma_{\vec{k}_c,\beta} = 1$ for $J_2 - J_3 < 0$. In the first Brillouin zone, $\vec{k}_c = (\pm\frac{4\pi}{3}, 0, 0)$ or $(\pm\frac{2\pi}{3}, \pm\frac{2\pi}{\sqrt{3}}, 0)$ for $J_2 - J_3 > 0$ and $\vec{k}_c = (0,0,0)$ for $J_2 - J_3 < 0$. When the effects of $p_{\sigma,\vec{\Delta}}$ and $q_{\sigma,\vec{\Delta}}$ are included, the spectra change little and the energy gap still appears at the same $\vec{k}_c$. However, the degeneracy of the spectra is lifted and the component $\omega_{\vec{k},0}$ becomes the lowest. This artifact may be remedied by using the operators of t_α $(\alpha = x, y, z)$ instead of $t_{0,\pm 1}$, as suggested by Brenig and Becker.[17] As shown by Gopalan *et al.*[18] in studying the spin ladders, the three triplet modes are degenerate when the corrections of the four operator terms are included by introducing the mean fields $P = P_\alpha = \langle t^\dagger_{i\alpha} t_{i+1\alpha} \rangle$ and $Q = Q_\alpha = \langle t^\dagger_{i\alpha} t^\dagger_{i+1\alpha} \rangle$. P_z and Q_z are equivalent to the present $p_{0,\vec{\Delta}}$ and $q_{0,\vec{\Delta}}$, respectively. Substituting $t^\dagger_x = -\frac{1}{\sqrt{2}}(t^\dagger_1 + t^\dagger_{-1})$ and $t^\dagger_y = \frac{i}{\sqrt{2}}(t^\dagger_1 - t^\dagger_{-1})$ into P and Q and comparing with the mean fields $p_{\sigma,\vec{\Delta}} = \langle t^\dagger_{\vec{r},\sigma} t_{\vec{r}+\vec{\Delta},\sigma} \rangle$, $q_{\sigma,\vec{\Delta}} = \langle t^\dagger_{\vec{r},\sigma} t^\dagger_{\vec{r}+\vec{\Delta},\bar{\sigma}} \rangle$, $\sigma = \pm 1$, we find that such terms as $\langle t^\dagger_{\vec{r},\sigma} t_{\vec{r}+\vec{\Delta},\bar{\sigma}} \rangle$ and $\langle t^\dagger_{\vec{r},\sigma} t^\dagger_{\vec{r}+\vec{\Delta},\sigma} \rangle$ are omitted in the p_σ (q_σ) terms. The effects of these terms are tiny since they describe the effects of two-magnon excitations. The difference between $\omega_{\vec{k},0}$ and $\omega_{\vec{k},\pm 1}$ is thus small. For example, inserting $J_1 = 0.01J_0$, $J_2 - J_3 = 0.05J_0$, and $J_3 = 0.3J_0$, we get the degenerate triplet gap as $\Delta_0 = \Delta_{\pm 1} = 0.798J_0$. When the effects of p and q are included, we have $\Delta_{\pm 1} = 0.797J_0$ and $\Delta_0 = 0.787J_0$. To study the splitting of the excitation spectra in the magnetic field and the various field-induced properties, it is more suitable to use the operators of $t_{0,\pm 1}$ for the moment. For simplicity, we will neglect $p_{\sigma,\vec{\Delta}}$ and $q_{\sigma,\vec{\Delta}}$ in the following calculations since their effects are small, just as shown in the spin ladder systems.[18]

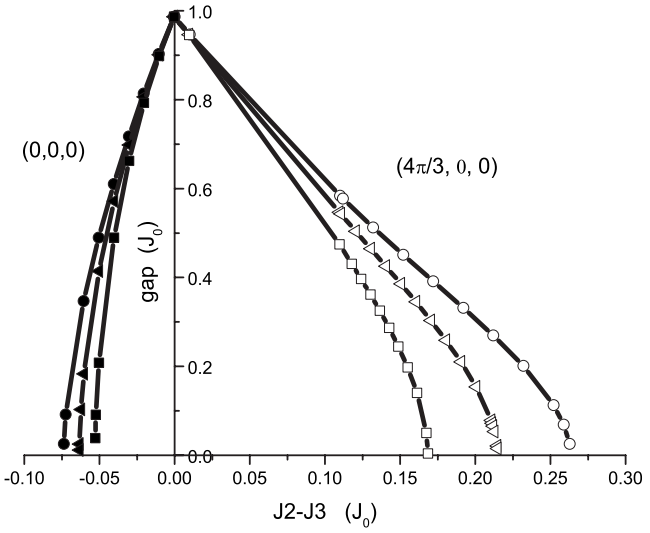

FIG. 2. Dependence of the triplet gap on $(J_2 - J_3)/J_0$. The curves with circles, triangles, and squares correspond to $J_3/J_0 = 0.1$, 0.2, and 0.3, respectively, and $J_1/J_0 = 0.01$. The energy gap is located at $\vec{k}_c = (4\frac{\pi}{3}, 0, 0)$ for $J_2 > J_3$ (white symbols) and at $\vec{k}_c = (0,0,0)$ for $J_2 < J_3$ (black symbols). When the energy gap vanishes at the critical $(J_2 - J_3)_c$, long-range order characterized by corresponding $\vec{k}_c$ appears.

In Fig. 2, we show the variations of the energy gap with $J_2 - J_3$ in units of J_0. For given J_1 and J_3, the energy gap goes to zero at a critical $(J_2 - J_3)_c$, denoting a transition from the gapped spin liquid state to ordered states. These ordered states can be described by the Bose-Einstein condensation of the corresponding magnons. For $(J_2 - J_3)_c > 0$, the magnons with $\vec{k}_c = (\frac{4\pi}{3}, 0, 0)$ or $(\frac{2\pi}{3}, \frac{2\pi}{\sqrt{3}}, 0)$ condense and the so-called three-sublattice 120° spin structure with different chirality is induced. For $(J_2 - J_3)_c < 0$, Bose-Einstein condensation of magnons occurs at $\vec{k}_c = (0,0,0)$ and we get a ferromagnetic state.

Along the line of $J_2 = J_3$, the excitation spectra are flat in the k_x-k_y plane, indicating the specific feature of quantum

phase transitions. For the special case of $J_2=J_3$ and $J_1=0$, Hamiltonian (1) reduces to

$$H=\frac{J_0}{2}\sum_{\vec{r}}\vec{\mathcal{S}}_{\vec{r}}^2+\frac{J_2}{2}\sum_{\vec{r}}\sum_{\alpha}\vec{\mathcal{S}}_{\vec{r}}\cdot\vec{\mathcal{S}}_{\vec{r}+\vec{\alpha}}-2NJ_0, \tag{6}$$

with $\vec{\mathcal{S}}_{\vec{r}}=\vec{S}_{\vec{r},1}+\vec{S}_{\vec{r},2}$, and N the number of dimers. It describes a system of combined spin $\vec{\mathcal{S}}_{\vec{r}}$'s interacting on a triangular lattice with $\mathcal{S}=0,1,2$. When J_0 is large enough, the system will be in the spin liquid state with every dimer in the singlet state; while when J_2 is very large, every dimer prefers to be in the state with $\mathcal{S}=2$ and the system will be in the three-sublattice 120° Néel state. So there must exist a quantum phase transition from the spin liquid state to the Néel state if there is no other intermediate state(s) between them. Ignoring the possible intermediate state, we can estimate the critical point by $\frac{J_0}{2}\Sigma_{\vec{r}}\langle\vec{\mathcal{S}}_{\vec{r}}^2\rangle+\frac{J_2}{2}\Sigma_{\vec{r}}\Sigma_{\alpha}\langle\vec{\mathcal{S}}_{\vec{r}}\cdot\vec{\mathcal{S}}_{\vec{r}+\vec{\alpha}}\rangle=0$. Recalling the results from the spin wave theory,[19] we get $J_{2c}=\frac{1}{3}\frac{\mathcal{S}+1}{\mathcal{S}+c}J_0$. With $c=0.218\,412$ and $\mathcal{S}=2$, we have $J_{2c}=0.4508J_0$.

IV. MAGNETIC AND THERMODYNAMIC PROPERTIES

We now study the thermodynamic properties of model (1) in an external magnetic field and the phase diagram in the H-T plane in connection with the experimental results on $Ba_3Mn_2O_8$. As shown in Eqs. (4), the triplet excitations split under the applied magnetic field and one component decreases with increasing magnetic field. At a critical magnetic field h_{c1}, the energy gap goes to zero. For any larger magnetic field $h>h_{c1}$, the magnons with momentum k_c will condense and induce long-range order in the plane perpendicular to the magnetic field. With a condensed density $n(h,T)=\frac{1}{N}\frac{4s^2/3\mathcal{J}_{\vec{k}_c}+\mu}{\omega_{\vec{k}_c,0}}\langle\alpha_{\vec{k},1}^{\dagger}\alpha_{\vec{k},1}\rangle$ extracted, the self-consistent equations become

$$s^2=\frac{5}{2}-\frac{1}{N}\sum_{\vec{k}}\frac{\frac{4}{3}s^2\mathcal{J}_{\vec{k}}+\mu}{\omega_{\vec{k},0}}\sum_{\sigma=\pm1,0}\left(\frac{1}{2}+n_{\vec{k},\sigma}\right)-n(h,T),$$

$$\mu=J_0-\frac{1}{N}\sum_{\vec{k}}\frac{\frac{4}{3}\mu\mathcal{J}_{\vec{k}}}{\omega_{\vec{k},0}}\sum_{\sigma=\pm1,0}\left(\frac{1}{2}+n_{\vec{k},\sigma}\right)-\frac{\frac{4}{3}\mu\mathcal{J}_{\vec{k}_c}}{\frac{4}{3}s^2\mathcal{J}_{\vec{k}_c}+\mu}n(h,T),$$

$$m=\frac{1}{N}\sum_{\vec{k}}\sum_{\sigma=\pm1}\sigma n_{\vec{k},\sigma}+\frac{\omega_{\vec{k}_c,0}}{\frac{4}{3}s^2\mathcal{J}_{\vec{k}_c}+\mu}n(h,T), \tag{7}$$

with $\omega_{\vec{k}_c,1}=0$. Here, $p_{\sigma,\Delta}$ and $q_{\sigma,\Delta}$ are neglected. The field-induced magnetization in the perpendicular plane is $m_x=\sqrt{\frac{4}{3}s^2\mu n(h,T)/\{\mu-\frac{4}{3}s^2[3(J_2-J_3)+J_1]\}}$.

Before proceeding to numerically solve the self-consistent equations, we need to determine the exchange coupling constants J_i $(i=0,1,2,3)$ in relation to $Ba_3Mn_2O_8$. Assuming a helical incommensurate structure characterized by an angle α in the basal plane and using the mean-field approximation, Uchida *et al.*[13] obtained $J_0=17.4$ K and $2(J_2+J_3)+J_1=8.3$ K. Furthermore, the angle α satisfies $(J_2-J_3)(4\cos\alpha+2\cos 2\alpha)-J_1(2\cos\alpha+1)=-3.7$ K. However, two other conditions are required to determine the individual values of J_i $(i=1,2,3)$. In our calculations with the simplified geometry, we have $\alpha=\frac{2\pi}{3}$. Keeping $T_c=0.85$ K at $H=17$ T at the top of the T-H curve,[14] we try sets of J_i $(i=1,2,3)$ and extract these parameters as $J_1/J_0=8.04\times10^{-3}$, $J_2/J_0=0.153$, and $J_3/J_0=8.16\times10^{-2}$. With these parameters, we calculate the magnetization, the specific heat, and the phase diagram in the T-H plane. The effects of the geometry, especially the incommensurability, will be discussed later.

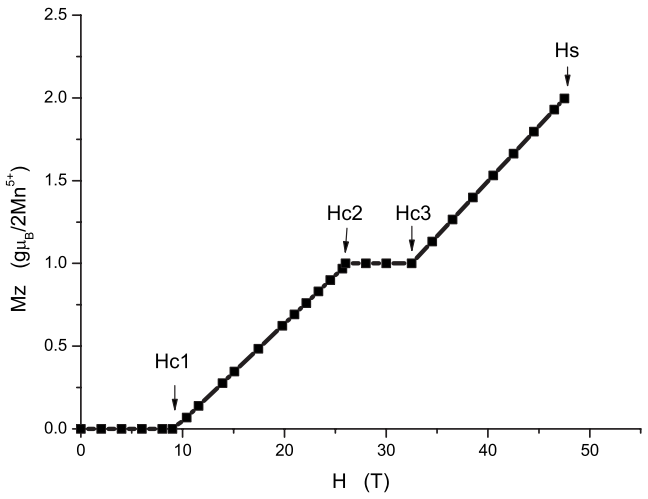

FIG. 3. Dependence of the uniform magnetization on external magnetic fields at vanishing temperatures.

The magnetization curve at zero temperature is shown in Fig. 3. The calculated $H_{c1}=9.5$ T agrees well with the experimental 9.2 T. When $H>H_{c1}$, the magnetization increases linearly H_{c2}, where a magnetization plateau of $\frac{1}{2}m_s$ appears and all the dimers are in the triplet state of $|t_1\rangle$. To study this state as well as the magnetization process at higher magnetic field, we have to consider the quintuplets. Since the two lowest states are now $|t_1\rangle$ and $|q_2\rangle$, we project all the other states in the bond-operator representation. Taking $\langle t_1^{\dagger}\rangle=\langle t_1\rangle=t$, it is easy to get the diagonalized Hamiltonian as $H=Ne_0+\Sigma_{\vec{k}}n_{\vec{k},q}\omega_{\vec{k},q}$, with e_0 a constant independent of $\vec{k}$ and $\omega_{\vec{k},q}=t^2\mathcal{J}_{\vec{k}}+3J_0+\mu-2h+(t^2+2n_q)J$. The lowest excitation (the gap) is also located at the same $\vec{k}_c$. The new self-consistent equations are

$$t^2=1-n_q(h,T)-\frac{1}{N}\sum_{\vec{k}}n_{\vec{k},q,2},$$

$$\mu=-J_0+h-\frac{1}{2}t^2J-n_q(h,T)(J+\mathcal{J}_{\vec{k}_c})-\frac{1}{N}\sum_{\vec{k}}n_{\vec{k},q,2}(J+\mathcal{J}_{\vec{k}}),$$

$$n_{q,2}=n_q(h,T)+\frac{1}{N}\sum_{\vec{k}}n_{\vec{k},q,2}. \tag{8}$$

When $\omega_{\vec{k}_c,q}>0$ and $n_q(h,T)=0$, we get a gapped spin liquid state and, correspondingly, a $\frac{1}{2}m_s$ magnetization plateau be-

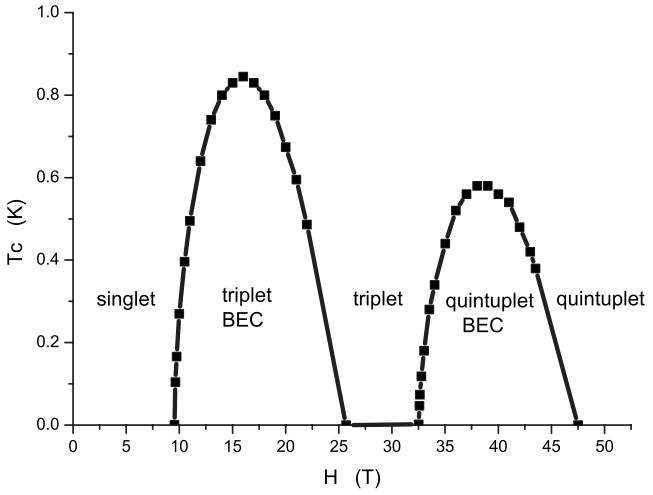

FIG. 4. *H-T* phase diagram of spin-1 dimers on hexagonal dimer lattices.

tween H_{c2} and H_{c3}. The calculated $H_{c2}=25.7$ T and $H_{c3}=32.5$ T, agreeing well with the experimental $H_{c2}=25.9$ T and $H_{c3}=32.3$ T. The state with $\omega_{\vec{k}_c,q}=0$ and $n_q(h,T)>0$ describes the BEC of the quintuplet magnons at $\vec{k}_c$ at $H_{c3}<H<H_s$. The field-induced magnetization in the perpendicular plane is $m_x'=\sqrt{t^2 n_q(h,T)}$. At $H_s=47.5$ T, all the dimers are in the state of $|q_2\rangle$ and the saturation magnetization is reached. The experimental $H_s=48$ T. The two slopes are calculated as $0.0588T^{-1}$ at $H_{c1}<H<H_{c2}$ and $0.0664T^{-1}$ at $H_{c3}<H<H_s$, which agree well with Uchida *et al.*'s mean-field results $2g\mu_B/(\frac{4}{3}a+b)=0.0593T^{-1}$ and $2g\mu_B/(a+b)=0.0667T^{-1}$.

In the regions of $H_{c1}<H<H_{c2}$ and $H_{c3}<H<H_s$, where Bose-Einstein condensation of magnons occurs, there exists a critical temperature T_c below which the field-induced transverse magnetization forms the 120° three-sublattice structure. The critical temperature T_c as a function of H is shown in Fig. 4. The left part (part I) with $H_{c1}<H<H_{c2}$ is calculated from Eqs. (7) and the right part (part II) from Eqs. (8). Part I agrees well with the experimental curve.[14] However, we do not observe the splits of H_{c1} and H_{c2} at zero temperature. Part II has a similar shape to the part I but with lower T_c. Its experimental counterpart is absent at present because of the too high magnetic field. Near H_{c1} and H_{c3}, we fit the results with $T_c \propto (H-H_c)^\alpha$ and get $\alpha=0.652$ near H_{c1} and $\alpha'=0.645$ near H_{c3}, very close to the value $\frac{2}{3}$ from the three-dimensional *XY* model. The experimental $\alpha=0.39$ near H_{c1} is a little smaller. We believe this discrepancy will be reduced or disappear with a more precisely determined H_{c1} and a narrower temperature region. The critical exponent has been extensively studied through different theoretical methods such as Bose-Einstein Hartree-Fock theory,[6,7] bond-operator mean-field theory,[9] and quantum Monte Carlo simulations[10,11] on different models and the same result of about $\frac{2}{3}$ has been given. Experimentally, although the reported value is discrete in different materials, it also begins to converge to $\frac{2}{3}$, for example, in $TlCuCl_3$, $BaCuSi_2O_6$ and $NiCl_2\cdot 4SC(NH_2)_2$.[20]

In Figs. 5(a) and 5(b), we show the decrease of the field-induced staggered magnetization with increasing temperatures at fixed magnetic field. The magnetization vanishes at the critical temperature T_c. The results at $H_{c1}<H<H_{c2}$ [Fig. 5(a)] are from Eqs. (7) and those at $H_{c3}<H<H_s$ [Fig. 5(b)] from Eqs. (8). The magnetic field dependences of the staggered magnetization at zero temperature are presented in Fig. 6.

In Figs. 7(a) and 7(b), we show the T dependence of the specific heat at different magnetic fields. At fixed H, a peak is obtained at the critical temperature T_c. The height and the location of the peak move up with increasing field when $H<(H_{c1}+H_{c2})/2$. These results agree well with the experiments. When $H>(H_{c1}+H_{c2})/2$, our calculated $C(T)$ curve

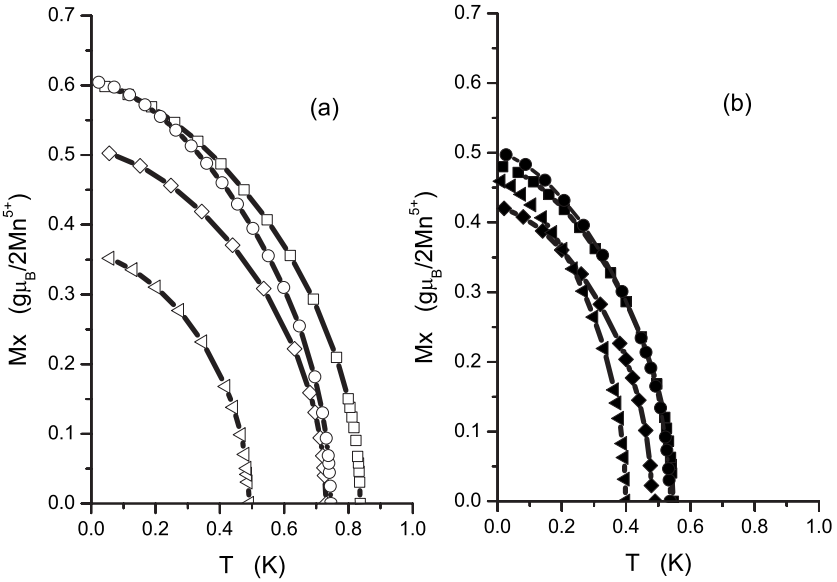

FIG. 5. Temperature dependence of the staggered magnetization at different magnetic fields. The magnetic fields are fixed at (a) $H=11$ (triangles), 13 (diamonds), 16 (squares), and 19 T (circles) and (b) $H=36$ (triangles), 38 (squares), 40 (circles), and 43 T (diamonds).

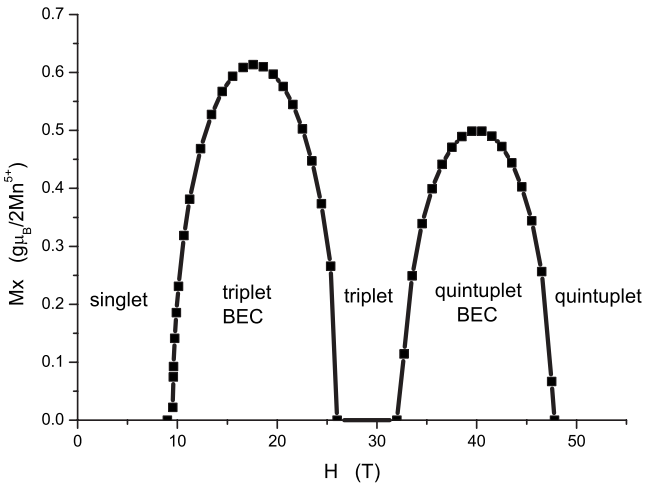

FIG. 6. Magnetic field dependence of the staggered magnetization at zero temperature.

also shows peaks with the right locations but incorrect height. We do not show them here. There is no report of measurements of specific heat at $H > H_{c2}$ at present.

V. FURTHER DISCUSSIONS ON $Ba_3Mn_2O_8$

With model Hamiltonian (1) as well as the simplified geometry, we have interpreted the experiments on $Ba_3Mn_2O_8$ quite well. We now consider the effects of the true lattice structure of $Ba_3Mn_2O_8$ with the double-layered triangular lattices stacked along the c axis with a periodicity of 3. Correspondingly, we have to replace J, $\gamma_{\vec{k},\beta}$, and $\mathcal{J}_{\vec{k}}$ with $J' = 3J_1 + 6(J_2 + J_3)$, $\gamma'_{\vec{k},\beta} = \frac{2}{3}\cos\left(\frac{1}{2}k_x a\right)\cos\left(\frac{1}{2\sqrt{3}}k_y a + k_z c\right) + \frac{1}{3}\cos\left(-\frac{1}{\sqrt{3}}k_y a + k_z c\right)$, and $\mathcal{J}'_{\vec{k}} = 6(J_2 - J_3)\gamma_{\vec{k},\alpha} - 3J_1\gamma'_{\vec{k},\beta}$. When $J_2 - J_3 > 0$ and $J_1 > 0$, the excitation spectra has an energy gap located at $\vec{k}'_c = \left(\frac{4}{3}\pi - \delta, 0, 0\right)$ or $\left(\frac{2}{3}\pi - \delta, \frac{2}{\sqrt{3}}\pi, -\frac{\pi}{3}\right)$. Hence, the Bose-Einstein condensation of the corresponding magnons will induce an incommensurate long-range order in the basal plane. The deviation from the 120° configuration along [1, 0, 0], or the incommensurability, is determined by $\delta \approx J_1/\sqrt{3}(J_2 - J_3)$. With the above extracted J_i $(i = 1, 2, 3)$, we get $\delta \approx 0.02\pi$. An experimentally measured δ is needed.

Two peaks (shoulders) were observed in the $C(T)$ curve at $H = 12$ T ($H = 24$ T) and two H_{c1}'s and two H_{c2}'s were suggested in the H-T phase diagram.[14] Similar behavior was also observed in other triangular magnets such as $CsFeBr_3$ (Ref. 21) and $CsFeCl_3$.[22] The origin is still in controversy. Considering the incommensurability discussed above, we guess the separation of H_c's is related to the incommensurate-commensurate transition, which deserves more detailed investigation, both experimentally and theoretically.

In general, there exist anisotropic terms such as DS_z^2 and $E(S_x^2 - S_y^2)$ for $S \geqslant 1$ spin systems. In $Ba_3Mn_2O_8$, the electronic ground state of the Mn^{5+} ion with the $3d^2$ configuration is ^3F, which splits into three states of Γ_4, Γ_5, and Γ_2. The nondegenerate Γ_2 state has the lowest energy and gives an effective $S = 1$ spin. Experimentally,[13] no effect of the E term was observed and the D term was estimated as $D \sim 0.1(g\mu_B) \sim 0.133$ K $\sim 7.6 \times 10^{-3} J_0$, much smaller than the intrabilayer interactions J_0, J_2, and J_3, but comparable to the interbilayer interaction J_1. The inclusion of the D term will not change our results greatly, since the main features of $Ba_3Mn_2O_8$ are determined by the bilayer structure and the spin exchange interactions inside it. Theoretically, if a considerable D term is considered in the model of Hamiltonian (1), the singlet and the quintuplet will mix in the bond-operator representation.[16] The ground state will then have an important component of quintuplets. The excitation spectra, and furthermore the quantum phase transitions, will be rich and interesting.

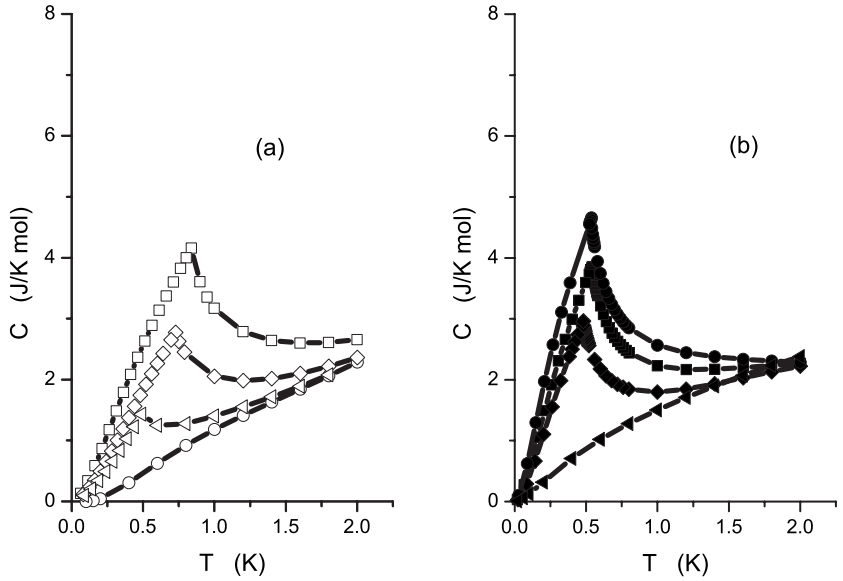

FIG. 7. Temperature dependence of heat capacities at (a) $H = 9$ (circles), 11 (triangles), 13 (diamonds), and 16 T (squares) and (b) $H = 32.5$ (triangles), 36 (diamonds), 38 (squares), and 40 T (circles).

VI. SUMMARY

In summary, we applied the bond-operator theory under the mean-field approximation to study coupled spin-1 dimers on stacked triangular lattices and interpreted the experimental results of $Ba_3Mn_2O_8$. The quantum phase transitions from the gapped spin liquid state to some ordered states are discussed by studying the changes of the energy gap with J_i and the Bose-Einstein condensation of related magnons. The transverse component of dimer spins aligns parallel when $J_2-J_3<0$ and in the 120° configuration when $J_2-J_3>0$. While at $J_2=J_3$ and $J_1=0$, a quantum phase transition from the spin liquid state to the triangularly ordered quintuplets is estimated at $J_2=0.4508J_0$ if there is no intermediate state(s) between them. With the extracted exchange coupling constants $J_1/J_0=8.04\times10^{-3}$, $J_2/J_0=0.153$, and $J_3/J_0=8.16\times10^{-2}$, the magnetization curve, the H-T phase diagram, and the temperature dependence of heat capacities are calculated. These results agree well with the experimental results on $Ba_3Mn_2O_8$. The incommensurability is estimated as $\delta=0.02\pi$.

ACKNOWLEDGMENTS

We acknowledge financial support by Natural Science Foundation of China and 973-project under Grants No. 2006CB921300 and No. 2006CB921400.

[1] T. Matsubara and H. Matsuda, Prog. Theor. Phys. **16**, 569 (1956).
[2] I. Affleck, Phys. Rev. B **41**, 6697 (1990); **43**, 3215 (1991).
[3] T. Giamarchi and A. M. Tsvelik, Phys. Rev. B **59**, 11398 (1999).
[4] A. Oosawa, H. Ishii, and H. Tanaka, J. Phys.: Condens. Matter **11**, 265 (1999); A. Oosawa, H. Aruga Katori, and H. Tanaka, Phys. Rev. B **63**, 134416 (2001); N. Cavadini, G. Heigold, W. Henggeler, A. Furrer, H.-U. Güdel, K. Krämer, and H. Mutka, *ibid.* **63**, 172414 (2001); N. Cavadini, Ch. Ruegg, A. Furrer, H. U. Gudel, K. Kramer, H. Mutka, and P. Vorderwisch, *ibid.* **65**, 132415 (2002); C. Rüegg, N. Cavadini, A. Furrer, H.-U. Gudel, K. Kramer, H. Mutka, A. Wildes, K. Habicht, and P. Vorderwisch, *ibid.* **423**, 62 (2003); E. Ya. Sherman, P. Lemmens, B. Busse, A. Oosawa, and H. Tanaka, Phys. Rev. Lett. **91**, 057201 (2003); C. Rüegg, A. Furrer, D. Sheptyakov, T. Strässle, K. W. Krämer, H.-U. Güdel, and L. Mélési, *ibid.* **93**, 257201 (2004); O. Vyaselev, M. Takigawa, A. Vasiliev, A. Oosawa, and H. Tanaka, *ibid.* **92**, 207202 (2004); C. Rüegg, B. Normand, M. Matsumoto, C. Niedermayer, A. Furrer, K. W. Krämer, H.-U. Güdel, Ph. Bourges, Y. Sidis, and H. Mutka, *ibid.* **95**, 267201 (2005).
[5] Y. Sasago, K. Uchinokura, A. Zheludev, and G. Shirane, Phys. Rev. B **55**, 8357 (1997); M. Jaime, V. F. Correa, N. Harrison, C. D. Batista, N. Kawashima, Y. Kazuma, G. A. Jorge, R. Stern, I. Heinmaa, S. A. Zvyagin, Y. Sasago, and K. Uchinokura, Phys. Rev. Lett. **93**, 087203 (2004); S. E. Sebastian, P. A. Sharma, M. Jaime, N. Harrison, V. Correa, L. Balicas, N. Kawashima, C. D. Batista, and I. R. Fisher, Phys. Rev. B **72**, 100404(R) (2005); S. E. Sebastian, N. Harrison, C. D. Batista, L. Balicas, M. Jaime, P. A. Sharma, N. Kawashima, and I. R. Fisher, Nature (London) **441**, 617 (2006); C. Rüegg, D. F. McMorrow, B. Normand, H. M. Rønnow, S. E. Sebastian, I. R. Fisher, C. D. Batista, S. N. Gvasaliya, Ch. Niedermayer, and J. Stahn, Phys. Rev. Lett. **98**, 017202 (2007).
[6] T. Nikuni, M. Oshikawa, A. Oosawa, and H. Tanaka, Phys. Rev. Lett. **84**, 5868 (2000).
[7] G. Misguich and M. Oshikawa, J. Phys. Soc. Jpn. **73**, 3429 (2004).
[8] M. Matsumoto, B. Normand, T. M. Rice, and M. Sigrist, Phys. Rev. Lett. **89**, 077203 (2002).
[9] H.-T. Wang, B. Xu, and Y. Wang, J. Phys.: Condens. Matter **18**, 4719 (2006).
[10] S. Wessel, M. Olshanii, and S. Haas, Phys. Rev. Lett. **87**, 206407 (2001); O. Nohadani, S. Wessel, B. Normand, and S. Haas, Phys. Rev. B **69**, 220402(R) (2004).
[11] N. Kawashima, J. Phys. Soc. Jpn. **73**, 3219 (2004).
[12] M. Uchida, H. Tanaka, M. I. Bartashevich, and T. Goto, J. Phys. Soc. Jpn. **70**, 1790 (2001).
[13] M. Uchida, H. Tanaka, H. Mitamura, F. Ishikawa, and T. Goto, Phys. Rev. B **66**, 054429 (2002).
[14] H. Tsujii, B. Andraka, M. Uchida, H. Tanaka, and Y. Takano, Phys. Rev. B **72**, 214434 (2005).
[15] S. Sachdev and R. N. Bhatt, Phys. Rev. B **41**, 9323 (1990).
[16] Han-Ting Wang, H. Q. Lin, and Jue-Lian Shen, Phys. Rev. B **61**, 4019 (2000).
[17] W. Brenig and K. W. Becker, Phys. Rev. B **64**, 214413 (2001).
[18] S. Gopalan, T. M. Rice, and M. Sigrist, Phys. Rev. B **49**, 8901 (1994).
[19] Th. Jolicoeur and J. C. Le Guillou, Phys. Rev. B **40**, 2727 (1989).
[20] A. Paduan-Filho, X. Gratens, and N. F. Oliveira Jr., Phys. Rev. B **69**, 020405(R) (2004); V. S. Zapf, D. Zocco, B. R. Hansen, M. Jaime, N. Harrison, C. D. Batista, M. Kenzelmann, C. Niedermayer, A. Lacerda, and A. Paduan-Filho, Phys. Rev. Lett. **96**, 077204 (2006).
[21] Y. Tanaka, H. Tanaka, T. Ono, A. Oosawa, K. Morishita, K. Iio, T. Kato, H. A. Katori, M. I. Bartashevich, and T. Goto, J. Phys. Soc. Jpn. **70**, 3068 (2001); T. Makamura, T. Ishida, Y. Fujii, H. Kikuchi, M. Chiba, T. Kubo, Y. Yamamoto, and H. Hori, Physica B **329-333**, 864 (2003).
[22] M. Toda, Y. Fujii, S. Kawano, T. Goto, M. Chiba, S. Ueda, K. Nakajima, K. Kakurai, J. Klenke, R. Feyerherm, M. Meschke, H. A. Graf, and M. Steiner, Phys. Rev. B **71**, 224426 (2005).